Available online at www.sciencedirect.com

SciVerse ScienceDirect

Ceramics International 39 (2013) 2223–2229

CERAMICS INTERNATIONAL

www.elsevier.com/locate/ceramint

Microwave dielectric properties of SnO_2-doped $CaSiO_3$ ceramics

Qing Ma[a], Songping Wu[a,*], Chan Jiang[a], Jianhui Li[b]

[a]School of Chemistry and Chemical Engineering, South China University of Technology, Guangzhou 510641, China
[b]Shen Zhen Zhen Hua Ferrite and Ceramic Electronics Co., Ltd., Shenzhen 518109, China

Received 12 July 2012; received in revised form 23 August 2012; accepted 23 August 2012
Available online 6 September 2012

Abstract

SnO_2-doped $CaSiO_3$ ceramics were successfully synthesized by a solid-state method. Effects of different SnO_2 additions on the sintering behavior, microstructure and dielectric properties of $Ca(Sn_{1-x}Si_x)O_3$ ($x=0.5$–1.0) ceramics have been investigated. SnO_2 improved the densification process and expanded the sintering temperature range effectively. Moreover, Sn^{4+} substituting for Si^{4+} sites leads to the emergence of $Ca_3SnSi_2O_9$ phase, which has a positive effect on the dielectric properties of CaO–SiO_2–SnO_2 materials, especially the Qf value. The $Ca(Sn_{0.1}Si_{0.9})O_3$ ceramics sintered at 1375 °C possessed good microwave dielectric properties: $\varepsilon_r = 7.92$, $Qf = 58{,}000$ GHz and $\tau_f = -42$ ppm/°C. The $Ca(Sn_{0.4}Si_{0.6})O_3$ ceramics sintered at 1450 °C also exhibited good microwave dielectric properties of $\varepsilon_r = 9.27$, $Qf = 63{,}000$ GHz, and $\tau_f = -52$ ppm/°C. Thus, they are promising candidate materials for millimeter-wave devices.

Keywords: C. Dielectric properties; D. $CaSiO_3$ ceramics; D. $Ca_3SnSi_2O_9$; D. SnO_2 addition

1. Introduction

Microwave ceramic materials with low dielectric constant (ε_r) and high quality factor (Qf) have attracted numerous researches due to their wide application in wireless communication systems such as resonators, filters and antennas. The low ε_r value will minimize the cross-coupling effect with conducts, and a high quality factor will increase the selectivity. A near zero τ_f value is also required to ensure the stability of the frequency against temperature changes.

Low-K microwave ceramic materials include Al_2O_3, silicate and AB_2O_6 (A=Ca, Mg, Mn, Co, Ni, and Zn; B=Nb, and Ta) system. Al_2O_3 exhibits a low ε_r value of 10.5, and a high Qf value of 680,000 GHz. However, its τ_f value is low (−60 ppm/°C), and its sintering temperature is too high [1]. TiO_2 was added to Al_2O_3 in order to overcome these problems, and $0.9Al_2O_3$–$0.1TiO_2$ ceramics sintered at 1350 °C were found to show microwave dielectric properties of $\varepsilon_r = 12.4$, $Qf = 117{,}000$ GHz, and $\tau_f = 1.5$ ppm/°C [2].

In 1980, Pauling [3] reported that 50% of Si–O bonds in the SiO_4 tetrahedron were covalent bonds based on electronegativity difference between Si and O. Silicates [4], such as magnesium silicate ($MgSiO_3$), zinc silicate (Zn_2SiO_4) and wollastonite ($CaSiO_3$) with good performances are resources of microwave dielectric ceramics. The strong covalent bonds in the SiO_4 tetrahedron reduce the polarization, leading to the decreased ε_r value and increased Qf value.

$MgSiO_3$ was reported to have excellent dielectric properties: $\varepsilon_r = 6.7$, $Qf = 121{,}200$ GHz and $\tau_f = -17$ ppm/°C [5]. However, it has a very narrow sintering temperature region, and is easy to be powdered because of the inevitable phase transformation. Mg_2SiO_4 with low dielectric constant (6–7) and high Qf value (~241,500 GHz) was also reported, together with a temperature coefficient of −67 ppm/°C [6]. Zn_2SiO_4 ceramics, as another resource, which was synthesized through the sol–gel process, exhibited microwave dielectric properties: $\varepsilon_r = 6.6$, $Qf = 219{,}000$ GHz, $\tau_f = -61$ ppm/°C [7]. However, both Mg_2SiO_4 and Zn_2SiO_4 showed large negative τ_f values. Besides, Song et al. [8] found that $(Mg_{0.4}Zn_{0.6})_2SiO_4$ ceramics exhibited good dielectric characteristics: $\varepsilon_r = 6.6$, $Qf = 95{,}650$ GHz, $\tau_f = -60$ ppm/°C.

$CaSiO_3$ is also proven to be an important low dielectric constant material: $\varepsilon_r = 8.4$ (10 GHz), $Qf = 16{,}000$ GHz

*Corresponding author. Tel./fax: +86 20 87112897.
E-mail address: chwsp@scut.edu.cn (S. Wu).

0272-8842/$ - see front matter © 2012 Elsevier Ltd and Techna Group S.r.l. All rights reserved.
http://dx.doi.org/10.1016/j.ceramint.2012.08.066

(sintered at 1300 °C) [9]. However, the sintering temperature range of pure $CaSiO_3$ was very narrow and it was difficult to obtain dense $CaSiO_3$ ceramic materials by the traditional solid-state [10]. Wang et al. synthesized $CaSiO_3$ nanopowders by the sol–gel method, which achieved excellent dielectric properties: $\varepsilon_r=6.69$, $Qf=25{,}398$ GHz (sintered at 1320 °C) [11]. The dielectric constant, Qf and τ_f of $CaMgSi_2O_6$ ceramics sintered at 1290 °C were $\varepsilon_r=7.46$, $Qf=59{,}638$ GHz and $\tau_f=-46$ ppm/°C [12]. Wang et al. [13] found that the $0.88CaMgSi_2O_6$–$0.12CaTiO_3$ ceramic sintered at 1300 °C showed a relatively low-permittivity (9.42), high Qf value (52,800 GHz), and near-zero temperature coefficients (5.6 ppm/°C). Microwave properties of monoclinic $Ca_3SnSi_2O_9$ phase ceramics have also been reported: $\varepsilon_r=8.44$, $Qf=92{,}000$ GHz and $\tau_f=-60$ ppm/°C at 1500 °C [14].

Though various studies were conducted on silicates, microwave properties of SnO_2-substituted $CaSiO_3$ were seldom reported. The dielectric properties of $Ca(Sn_{1-x}Si_x)O_3$($x=0.5$–1.0) materials were analyzed based on the densification, the XRD patterns and the microstructure synthesis.

2. Experimental

The specimen powders were synthesized by the conventional solid-state method. $CaCO_3$, nano-SnO_2 particles ($d_{50}=0.2$ μm by a laser size distribution analyzer, Aladdin, Shanghai, China) and nano-SiO_2 (7 nm, Degussa, Auckland, New Zealand) were mixed with a proper element molar ratio of Ca:Sn:Si=1:(1−x):x ($x=0.5$–1.0), and then milled with zirconia balls for 4 h on a planetary milling machine (QM-3SP2, Zhenguang, Nanjing, China). The mixtures were dried, and calcined at 1000 °C for 2 h. The calcined ceramic powders were re-milled for 4 h, dried, and then pressed into cylindrical disks of 10 mm diameter and 5 mm thickness under a pressure of 300 MPa pressure isostatically with a hydrostatic press (YAW4106, Max press 300kN, China). The samples were sintered at 1250–1500 °C for 4 h in air with a high-temperature electric furnace (SSJ-1600, Shenjia Kiln, Luoyang, China).

The crystalline phases of specimen were analyzed by X-ray diffraction (XRD) (D8 ADVANCE, Bruker, Germany) with Cu Ka radiation. The microstructure observations of the ceramic surfaces were performed under a scanning electron microscope (SEM; LEO 1530 VP, Zeiss, Vertrieb Deutschland, Germany). The bulk densities of the sintered pellets were measured by the Archimedes method. The dielectric constants (ε_r) and the quality factor values (Qf) at microwave frequencies were measured by the Hakki–Coleman dielectric resonator method using a Network Analyzer (N5230 PNA-L, Agilent, Santa Clara, CA, USA). Temperature coefficient of resonant frequency (τ_f) was also measured by the same method with changing temperature from 25 to 75 °C, and was calculated by the following Eq. (1):

$$\tau_f = \frac{f_{75}-f_{25}}{f_{25}\times 50}\times 10^6 \quad (1)$$

where f_{75} and f_{25} represent the resonant frequency at 75 °C and 25 °C, respectively.

3. Results and discussion

3.1. Phase identification

The XRD patterns of $Ca(Sn_{1-x}Si_x)O_3$ ceramics (sintered at 1350 °C for 4 h) with x varying from 0.5 to 0.9 were shown in Fig. 1. According to the XRD patterns, triclinic $CaSiO_3$ phase (JCPDS no. 31-0300) was the main crystal phase, accompanied with a small amount of monoclinic $Ca_3SnSi_2O_9$ (JCPDS no. 46-0812). Moreover, the diffraction peaks of $CaSiO_3$ were weakened and those of $Ca_3SnSi_2O_9$ strengthened with increasing dosages of SnO_2. It indicates that the SnO_2 addition led to the appearance of $Ca_3SnSi_2O_9$ phase. Besides, the main peaks of $CaSiO_3$ (about 32°) shifted to lower angles as x increased, such as 31.7692°, 31.6871° and 31.6255° for $x=0.9$, 0.8 and 0.7, respectively. The possible reason was the lattices inflation deviated the larger ionic radius Sn^{4+} ions (0.069 nm) more than that of Si^{4+} ions (0.040 nm) [15]. When $x=0.5$ and 0.6, orthorhombic phase of $CaSnO_3$ (JCPDS no. 31-0312) appeared.

Fig. 2 shows the XRD patterns of $Ca(Sn_{0.1}Si_{0.9})O_3$ ceramics sintered at different temperatures (T_s) from 1250 °C to 1400 °C for 4 h. It is clearly seen that $CaSiO_3$ is the main crystal phase as the sintering temperatures vary from 1250 °C to 1375 °C, accompanied with a small amount of $Ca_3SnSi_2O_9$ as the second phase. However, the diffraction peaks for the $Ca_3SnSi_2O_9$ second phase disappeared when the specimen was sintered at 1400 °C. The diffraction peaks at 2θ of 12.196°, 29.503°, 30.043°, and 31.232° could be indexed to the characteristic peaks (100), (202), (113), and (023) of monoclinic $Ca_3SnSi_2O_9$ phase (JCPDS no. 46-0812), respectively, and peaks at 2θ

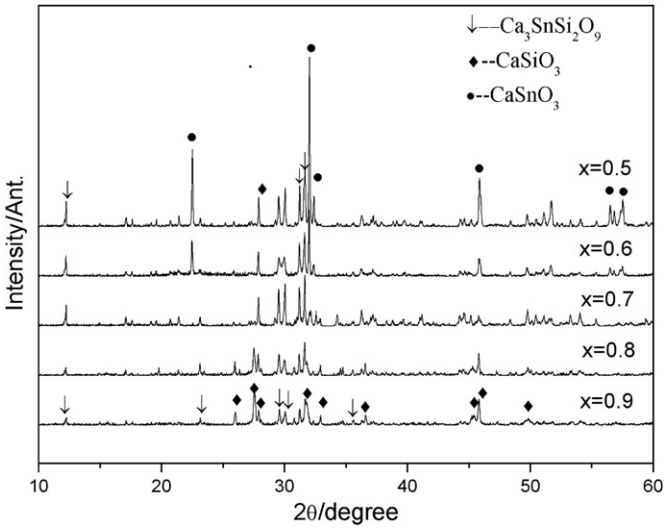

Fig. 1. XRD patterns of $Ca(Sn_{1-x}Si_x)O_3$ ceramics with various compositions at 1350 °C.

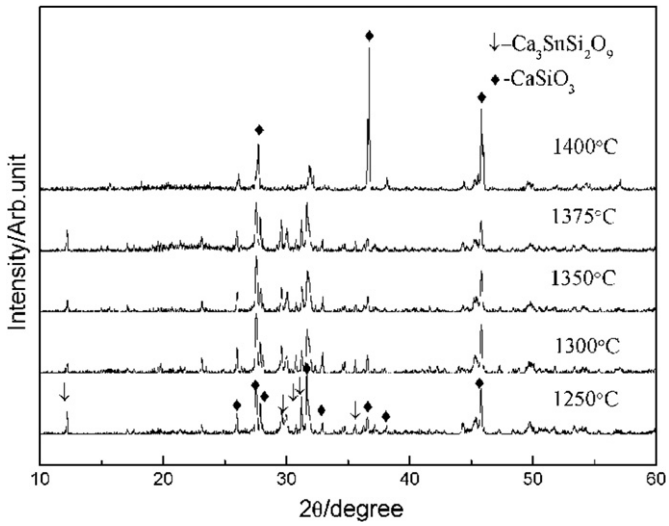

Fig. 2. XRD patterns of $Ca(Sn_{1-x}Si_x)O_3$ ($x=0.9$) ceramics sintered at various temperatures.

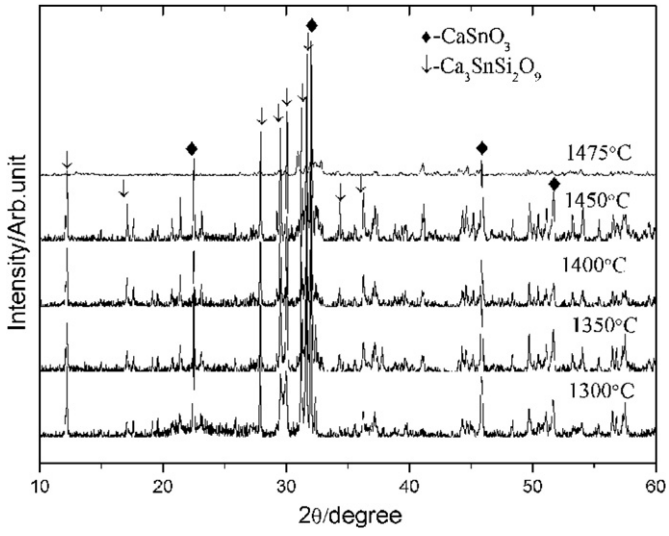

Fig. 3. XRD patterns of $Ca(Sn_{1-x}Si_x)O_3$ ($x=0.6$) ceramics sintered at various temperatures.

of 27.550°, 27.689°, 46.034°, 26.040°, 31.750°, 36.665°, and 45.353° could be indexed to the characteristic peaks (112), (122), (301), (120), (222), (008) and (128) of the triclinic $CaSiO_3$ phase (JCPDS no. 31-0300).

The XRD patterns of $Ca(Sn_{0.4}Si_{0.6})O_3$ ceramics sintered at different temperatures are given in Fig. 3 The $CaSnO_3$ phase (JCPDS no. 31-0312) and $Ca_3SnSi_2O_9$ phase (JCPDS no. 46-0812) varied to be the main crystal phase, with a small amount of $CaSiO_3$ phase. The amount of $CaSnO_3$ increased with the increase in sintering temperatures. The diffraction peaks at 2θ of 22.531°, 32.065°, 45.908°, 46.000°, and 57.620° could be indexed to the characteristic peaks (020), (121), (202), (040), and (123) of orthorhombic $CaSnO_3$ phase (JCPDS no. 31-0312), respectively.

The phase compositions with different x values at various sintering temperatures are shown in Fig. 4. The

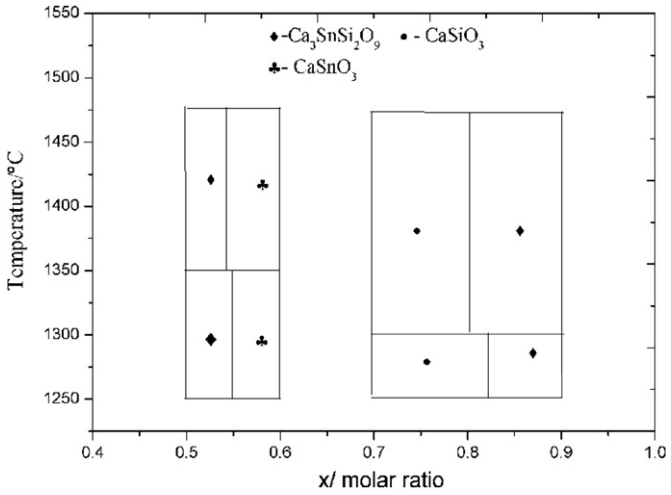

Fig. 4. Phase composition.

height of the strongest diffraction peak of every phase composition was compared to estimate the volume ratio of every phase in the specimens. The areas of squares roughly reflected the content of every phase. In the region of 1250–1450 °C, the phase compositions consisted of monoclinic $Ca_3SnSi_2O_9$ and triclinic $CaSiO_3$ for $x=0.7$–0.9; however, they were orthorhombic $CaSnO_3$ and $Ca_3SnSi_2O_9$ for $x=0.5$–0.6. As the temperature increased, the amount of specimens containing Tin element increased [16].

3.2. SEM studies

The microstructures of $Ca(Sn_{0.1}Si_{0.9})O_3$ ceramics sintered for 4 h at various temperatures are presented in Fig. 5. From Fig. 5(i), grain growth is not obvious and a porous microstructure developed due to low calcining temperature of 1250 °C, potentially degrading the microwave dielectric properties of specimens. The densification and grain size increased as the sintering temperature increased. The dense microstructure developed, and average grain size increased to 2.5 μm when sintered at 1375 °C, as given in Fig. 5(iii). Uniform fine-grain microstructures and clear grain boundaries can be observed. As the temperature was above 1400 °C, abnormal grain growth occurred, and obvious glass phase existed in grain boundaries, as exhibited in Fig. 5(iv).

Fig. 6 shows the microstructures of $Ca(Sn_{0.4}Si_{0.6})O_3$ ceramics sintered for 4 h at different temperatures. It can also be seen that the microstructures was closely correlated to the sintering temperatures. With SnO_2 addition, the sintering temperatures of materials improved clearly. The loose microstructure of $Ca(Sn_{0.4}Si_{0.6})O_3$ ceramics sintered at 1350 °C for 4 h was observed in Fig. 6(i). The pores of $Ca(Sn_{0.4}Si_{0.6})O_3$ ceramics almost disappeared at 1450 °C for 4 h. It can be observed from Fig. 6(iv) that a glass phase was formed when sintered at 1475 °C, implying the overheating of the sample.

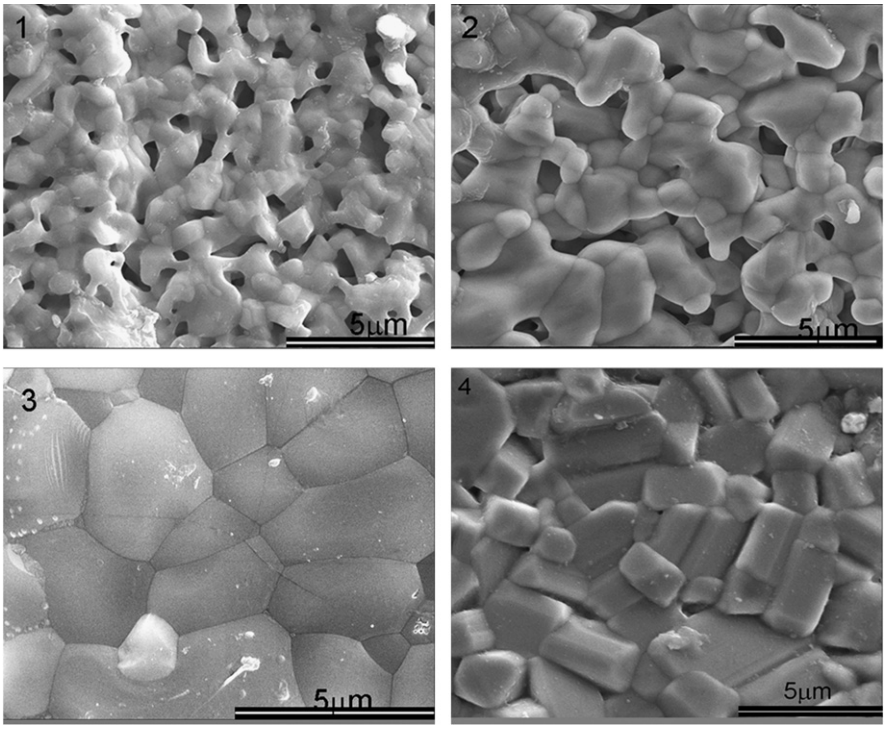

Fig. 5. SEM photographs of $Ca(Sn_{1-x}Si_x)O_3$ ($x=0.9$) ceramics sintered at: (i) 1300 °C, (ii) 1350 °C, (iii) 1375 °C, and (iv) 1400 °C.

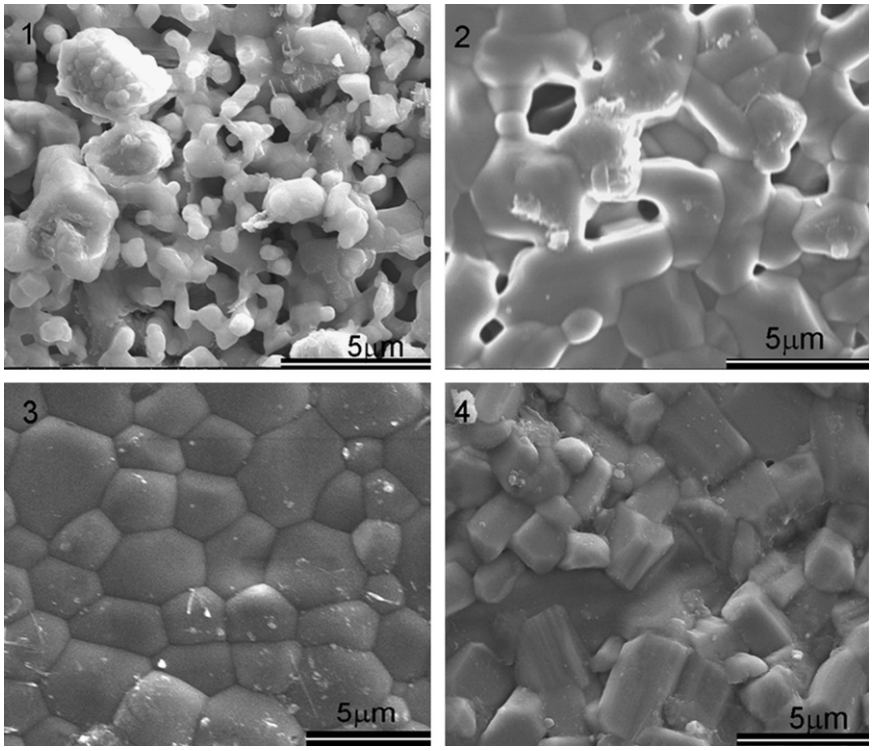

Fig. 6. SEM photographs of $Ca(Sn_{1-x}Si_x)O_3$($x=0.6$) ceramics sintered at: (i) 1350 °C, (ii) 1400 °C, (iii) 1450 °C, and (iv) 1475 °C.

3.3. Microwave dielectric properties

Fig. 7(i) shows the relative densities of the $Ca(Sn_{1-x}Si_x)O_3$ ceramics with $0.5 \le x \le 0.9$ sintered at 1250–1475 °C for 4 h. Generally, with the sintering temperatures increasing, the relative density would increase and get to a maximum value. For $Ca(Sn_{0.1}Si_{0.9})O_3$ ceramics, the value of relative density at 1250 °C was low (57.98%), then, it increased and reached

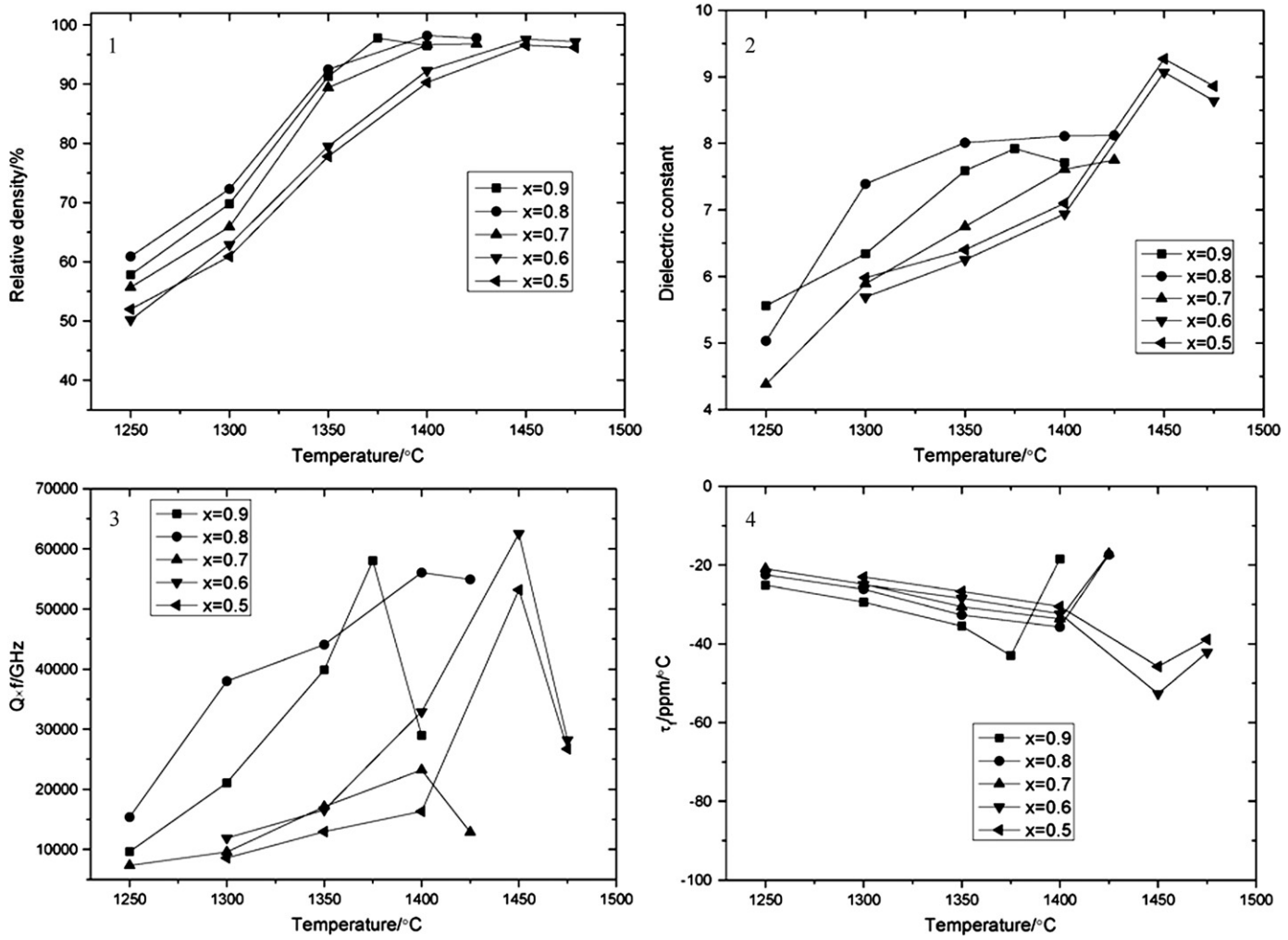

Fig. 7. (i) Relative density, (ii) ε_r , (iii) Qf , and (iv) τ_f of the $Ca(Sn_{1-x}Si_x)O_3$ ceramics with various compositions sintered at various temperatures for 4 h.

markedly to a maximum value of 97.55% at 1375 °C; beyond this temperature, it declined. The maximum relative density increased from 97.55% to 98.21% as x changed from 0.9 to 0.8. It could be ascribed to the phases change with different amounts of SnO_2 additions. The maximum relative density of $Ca(Sn_{0.4}Si_{0.6})O_3$ ceramics sintered at 1475 °C was 98.1%. The increase in relative density may be caused by the decrease in the number of pores and the uniform grain growth, as presented in Figs. 5 and 6.

The dielectric constants (ε_r) and Qf of the $Ca(Sn_{1-x}Si_x)O_3$ ceramics with different additions of SnO_2 sintered at various temperatures were illustrated in Fig. 7(ii, iii). The relationship between dielectric properties and the sintering temperatures is consistent with that between the relative density and the sintering temperatures. Microwave dielectric losses, including intrinsic and extrinsic loss, are affected by many factors. Intrinsic loss is associated with the vibration modes of the lattice. Extrinsic loss is associated with the density, porosity, second phases, impurities, oxygen vacancies, grain size, and internal strain and lattice defects [17,18]. The specimens with different x presented different trends, which were inferred to be affected by the different phases.

Dielectric constants are dependent on the ionic polarization [19] and microstructures. Generally, a higher density is associated with low porosity and a higher dielectric constant. For $Ca(Sn_{0.1}Si_{0.9})O_3$ ceramics, the ε_r value was low (5.56) when sintered at 1250 °C; however, it increased to a maximum value of 7.92 (at 14.94 GHz) for the specimen sintered at 1375 °C. The Qf value of $Ca(Sn_{0.1}Si_{0.9})O_3$ ceramics sintered at 1250 °C was very low (6600 GHz) due to the low density and porous microstructures, as shown in Fig. 7(iii) and it increased considerably to a maximum value of 58,000 GHz for the specimens sintered at 1375 °C, which had a strong correlation with the grain size. Compared with XRD patterns, the decreased Qf value at 1400 °C may be caused by the formation of defective grain boundaries due to overfiring.

The ε_r value of $Ca(Sn_{0.4}Si_{0.6})O_3$ ceramics sintered at 1300 °C for 4 h was low, probably due to the porous microstructure. It increased with increasing sintering temperatures, to a maximum dielectric constant of 9.27 (at 12.85 GHz) at 1450 °C; however, it decreased slightly at 1475 °C, which may have been caused by the presence of the defective grain boundaries due to overfiring.

Table 1
Microwave dielectric properties.

Samples	ε_r	Qf (GHz)	τ_f (ppm/°C)
$Ca(Sn_{0.1}Si_{0.9})O_3$ (1375 °C)	7.92	58,000	−42
$Ca(Sn_{0.1}Si_{0.9})O_3$ (1375 °C; calculated)	8.410	20,897.6	−29.6
$Ca(Sn_{0.4}Si_{0.6})O_3$ (1450 °C)	9.27	63,000	−52
$Ca(Sn_{0.4}Si_{0.6})O_3$ (1450 °C; calculated)	8.86	40,998.5	−33.9

$Ca(Sn_{0.4}Si_{0.6})O_3$ ceramics sintered at 1450 °C for 4 h showed the highest Qf value of 63,000 GHz. This is due to the high densification and large grain growth derived from a high sintering temperature, possessing a better ordering of the ions [20].

The τ_f values of $Ca(Sn_{1-x}Si_x)O_3$ ceramics sintered at various temperatures are shown in Fig. 7(iv). The τ_f value is related to the composition, the amounts of additives, and the second phase that present in the ceramics. Although different phases were found in the $Ca(Sn_{1-x}Si_x)O_3$ ceramics, all τ_f values of specimens ranged between −20 ppm/°C and −52 ppm/ °C, which are strongly dependent on calcination temperatures.

The experimental results of microwave dielectric properties of $Ca(Sn_{0.1}Si_{0.9})O_3$ (1375 °C) ceramics and $Ca(Sn_{0.4}Si_{0.6})O_3$ (1450 °C) ceramics are listed in Table 1. The variations of microwave dielectric properties are related to the change of SnO_2 compositions in the mixtures. The well-known general empirical model for multiphase ceramics was used to confirm the experimental results. The calculated dielectric constant, Qf value, and τ_f of the samples were obtained by the following equations [21,22]:

$$\ln\varepsilon = X_1 \ln\varepsilon_1 + X_2 \ln\varepsilon_2 \quad (2)$$

$$\frac{1}{Qf} = \frac{X_1}{Q_1 f_1} + \frac{X_2}{Q_2 f_2} \quad (3)$$

$$\tau_f = X_1\tau_{f1} + X_1\tau_{f2} \quad (4)$$

where X_1 and X_2 are the volume fractions of the $Ca_3SnSi_2O_9$ and $CaSiO_3$ or $CaSnO_3$, respectively; ε_1 and ε_2 are the dielectric constants of the $Ca_3SnSi_2O_9$ and $CaSiO_3$ or $CaSnO_3$; Q_1f_1 and Q_2f_2 are the Qf values of the $Ca_3SnSi_2O_9$ and $CaSiO_3$ or $CaSnO_3$; τ_{f1} and τ_{f2} are the τ_f of the $Ca_3SnSi_2O_9$ and $CaSiO_3$ or $CaSnO_3$, respectively. The volume fraction was calculated according to the XRD patterns. In our preliminary studies, microwave dielectric properties of $CaSnO_3$ were $\varepsilon_r = 9.08$, $Qf = 32{,}017$ GHz and $\tau_f = -20.73$ ppm/°C, and microwave dielectric properties of $CaSiO_3$ were $\varepsilon_r = 8.4$, $Qf = 16{,}000$ GHz and $\tau_f = -17.47$ ppm/°C. The experimental and calculated results are shown in Table 1. The calculated results are in agreement with the experimental results in the aspect of the phase change, which is emphasized in this article. The calculated quality factors of $Ca(Sn_{0.1}Si_{0.9})O_3$ and $Ca(Sn_{0.4}Si_{0.6})O_3$ are far lower than their experimental data. The possible reason is that the data we applied were not the ideal data because the specimens were not completely dense [9,11].

Even though the Qf value of the $Ca(Sn_{1-x}Si_x)O_3$ ceramics was lower than that for $MgSiO_3$ [5], Mg_2SiO_4 [6], Zn_2SiO_4 [7] or $Ca_3SnSi_2O_9$ [14] ceramics, it was higher than that of $CaSiO_3$ ceramics [9]. The $MgSiO_3$ ceramics have a very narrow temperature region (about 30 °C) and are easy to be powdered. The Zn_2SiO_4 ceramics exhibit a low Qf value (15,717 GHz at 1350 °C) when the conventional solid-state method is employed. The $Ca_3SnSi_2O_9$ ceramics have high sintering temperatures. In this work, we synthesized $Ca(Sn_{1-x}Si_x)O_3$ ceramics using the conventional solid-state method. The $Ca(Sn_{1-x}Si_x)O_3$ samples had wide sintering temperatures range (1350–1450 °C), which did not require accurate temperature controlling system. Within the wide sintering temperatures, phase compositions and microwave properties were stable, so we had more opportunities to choose the reaction conditions. These were all important factors for the applications.

Compared with $CaSiO_3$ ceramics, which have a narrow temperature and become more porous with increasing calcination temperature [9], the little SnO_2 addition is beneficial to improve the densification of specimens, and further increase the microwave dielectric properties.

4. Conclusion

The dielectric properties and microstructures of $Ca(Sn_{1-x}Si_x)O_3$ ($x = 0.5$–1.0) ceramics were investigated in order to clarify the effect of SnO_2 substitution on $CaSiO_3$ ceramics. SnO_2 is not detected in the ceramics, but $Ca_3SnSi_2O_9$ phase appeared. According to the XRD patterns, phases depend on the chemical composition. When $x = 0.7$–0.9, the main $CaSiO_3$ phase existed, accompanied with a little $Ca_3SnSi_2O_9$ phase. When $x = 0.5$–0.6, there was second phase of $CaSnO_3$. For $Ca(Sn_{0.4}Si_{0.6})O_3$ ceramics, a dense microstructure was developed at 1450 °C, which had a high relative density of >97%. Microwave dielectric properties of $Ca(Sn_{0.4}Si_{0.6})O_3$ sintered at 1450 °C for 4 h were obtained as follows: $\varepsilon_r = 9.27$, $Qf = 53{,}000$ GHz and $\tau_f = -52$ ppm/°C. High-density $Ca(Sn_{0.1}Si_{0.9})O_3$ ceramics sintered at 1375 °C for 4 h had a relative density of 97%, a dielectric constant of 7.92, a Qf of 58,000 GHz, and a temperature coefficient of resonant frequency (τ_f) of −42 ppm/°C. $Ca(Sn_{0.1}Si_{0.9})O_3$ ceramics have a wide sintering temperature and high quality factor. They could be considered as promising candidate microwave/millimeter-wave ceramic materials.

Acknowledgment

This work was supported by the Guangdong-Hong Kong Technology Cooperation Funding Scheme (TCFS) under Grant 2010A090604002 and State Key Laboratory of New Ceramic and Fine Processing, Tsinghua University.

References

[1] H.P. Sun, Q.L. Zhang, H. Yang, J.L. Zou, $Ca_{1-x}Mg_x)SiO_3$: a low-permittivity microwave dielectric ceramic system, Materials Science and Engineering B 138 (2007) 46–50.
[2] Q.L. Zhang, H. Yang, H.P. Sun, A new microwave ceramic with low-permittivity for LTCC applications, Journal of the European Ceramic Society 28 (2008) 605–609.
[3] L. Pauling, The nature of silicon–oxygen bonds, American Mineralogist 65 (1980) 321–323.
[4] K.X. Song, X.M. Chen, X.C. Fan, Effects of Mg/Si ratio on microwave dielectric characteristics of forsterite ceramics, Journal of the American Ceramic Society 90 (6) (2007) 1808–1811.
[5] M.E. Song, J.S. Kim, M.R. Joung, S. Nahm, Synthesis and microwave dielectric properties of $MgSiO_3$ ceramics, Journal of the American Ceramic Society 91 (8) (2008) 2747–2750.
[6] T. Tsunooka, M. Androu, Y. Higashida, Effects of TiO_2 on sinterability and dielectric properties of high-Q forsterite ceramics, Journal of the European Ceramic Society 23 (14) (2003) 2573–2578.
[7] Y. Guo, H. Ohsato, K.I. Kakimoto, Characterization and dielectric behavior of willemite and TiO_2-doped willemite ceramics at millimeter-wave frequency, Journal of the American Ceramic Society 26 (2006) 1827–18305.
[8] K.X. Song, X.M. Chen, C.W. Zheng, Microwave dielectric characteristics of ceramics in Mg_2SiO_4–Zn_2SiO_4 system, Ceramics International 34 (2008) 917–920.
[9] M. Valant, D. Suvorov, Glass-free low-temperature cofired ceramics: calcium germinates, silicates and tellurates, Journal of the European Ceramic Society 24 (2004) 1715–1719.
[10] R.P.S. Chakradhar, B.M. Nagabhushana, G.T. Chandrappa, K.P. Ramesh, J.L. Rao, Solution combustion derived nanocrystalline macroporous wollastonite ceramics, Materials Chemistry and Physics 95 (2006) 169–175.
[11] H.P. Wang, Q.L. Zhang, H. Yang, H.P. Sun, Synthesis and microwave dielectric properties of $CaSiO_3$ nanopowder by the sol–gel process, Ceramics International 34 (2008) 1405–1408.
[12] T. Joseph, M.T. Sebastian, Effect of glass addition on the microwave dielectric properties of $CaMgSi_2O_6$ ceramics, International Journal of Applied Ceramic Technology 7 (S1) (2010) E98–E106.
[13] H.P. Wang, S.Q. Xu, S.Y. Zhai, D.G. Deng, H.D. Ju, Effect of B_2O_3 additives on the sintering and dielectric behaviors of $CaMgSi_2O_6$ ceramics, Journal of Materials Science and Technology 26 (4) (2010) 351–354.
[14] S.P. Wu, D.F. Chen, Y.X. Mei, Q. Ma, Synthesis and microwave dielectric properties of $Ca_3SnSi_2O_9$ ceramics, Journal of Alloys and Compounds 521 (2012) 8–11.
[15] Y.C. Chen, M.D. Chen, Microwave dielectric properties of high quality factor $La(Mg_{0.5-x}Ca_xSn_{0.5})O_3$ ceramics, Journal of Physics and Chemistry of Solids 72 (2011) 1447–1451.
[16] V. Uvarov, I. Popov, Development and metrological characterization of quantitative X-ray diffraction phase analysis for the mixtures of clopidogrel bisulphate polymorphs, Journal of Pharmaceutical and Biomedical Analysis 46 (2008) 676–682.
[17] B.D. Silverman, Microwave absorption in cubic strontium titanate, Physical Review 125 (6) (1962) 1921–1930.
[18] W.S. Kim, T.H. Hong, E.S. Kim, K.H. Yoon, Microwave dielectric properties and far infrared reflectivity spectra of the $(Zr_{0.8}Sn_{0.2})TiO_4$ ceramics with additives, Japanese Journal of Applied Physics 37 (9) (1998) 3567–3571.
[19] Y. Tohdo, K. Kakimoto, H. Ohsato, H. Yamada, T. Okawa, Microwave dielectric properties and crystal structure of homologous compounds $ALa_4Ti_4O_{15}$ (A=Ba, Sr and Ca) for base station applications, Journal of the European Ceramic Society 26 (2006) 2039–2043.
[20] C.A. Lu, P. Lin, S.F. Wang, Microstructure and microwave dielectric properties of Li_2O–Nb_2O_5–ZrO_2 ceramics, Ceramics International 33 (2007) 1389–1393.
[21] A.E. Paladino, Temperature-compensated $MgTi_2O_5$–TiO_2 dielectrics, Journal of the American Ceramic Society 54 (1971) 168–169.
[22] F. Zhao, Z. Yue, Y. Lin, Z. Gui, L. Li, Phase relation and microwave dielectric properties of $xCaTiO_3$–$(1-x)TiO_2$–$3ZnTiO_3$ multiphase ceramics, Ceramics International 33 (2007) 895–900.